Lasers in Manufacturing Conference 2017

Incubation effect during laser irradiation of stainless steel with bursts of fs-pulses

Giuseppe Giannuzzi[a,b,*], Caterina Gaudiuso[a,b], Antonio Ancona[a,c], Pietro Mario Lugarà[a,b]

[a]*Istituto di Fotonica e Nanotecnologie (INF)-CNR U.O.S. Bari, via Amendola 173, I-70126 Bari, Italy*
[b]*Università degli Studi di Bari, Dipartimento Interuniversitario di Fisica, via Amendola 173, I-70126 Bari, Italy*
[c]*Departement of Engineering Science, University West, SE-46186 Trollhättan, Sweden*

Abstract

A thorough experimental investigation of the incubation effect influencing the ablation threshold during irradiation of steel samples with bursts of femtosecond laser pulses is presented. The bursts were generated using a cascade of birefringent crystals splitting pristine 650-fs laser pulses at 1030 nm wavelength into a tunable number of up to 32 sub-pulses with time separations in the picosecond range.
In Burst Mode (BM) processing we found that the threshold fluence strongly depends on the burst features.
These results have been compared to the case of multi-shot ablation in Normal Pulse Mode (NPM), finding that the models describing incubation in NPM are not applicable to BM. In particular, while the threshold fluence estimated in NPM has a unique value, in case of BM we found different values of ablation thresholds according to the total number of sub-pulses impinging on the sample surface.
Therefore, a modified incubation model has been introduced fitting the results obtained in BM, where the incubation coefficient depends on the burst composition.

Keywords: Ablation; Burst mode; Incubation; Femtosecond laser; Laser material processing

* Corresponding author. Tel.: (+39) 080 5442371.
E-mail address: giuseppe.giannuzzi@uniba.it

1. Introduction

The determination of the ablation threshold, i.e. the minimum energy density generating a permanent damage on the sample, and its dependence on irradiating conditions is of extreme importance for optics manufacturing industry, where knowing the damage threshold of optical elements and coatings is essential.

Incubation effect characterizes the laser ablation process when using trains of pulses in the so-called Normal Pulse Mode (NPM) and strongly influences the ablation threshold, leading to the reduction of the threshold fluence as a function of the number of impinging pulses. This effect was experimentally observed on several materials, such as metals, semiconductors, dielectrics (Nathala et al., 2016, Mannion et al., 2014, Bonse et al., 2002, Gómez et al., 2006, Machado et al., 2012) and its origin is attributed to an improvement of absorption of laser energy, thanks to the increase of the target surface roughness, pulse after pulse (Neuenschwander et al., 2013). One of the empirical models presented to explain this effect was originally proposed by Jee et al., 1988. It consisted in a power law where an incubation coefficient S was introduced for taking into account the dependence of threshold fluence on the number of pulses. In this model, S describes the strength of incubation effect: when S=1, there is no incubation and the ablation fluence stays constant irrespective the number of pulses. When S<1 incubation is observed and the lower the value of S, the more rapid is the reduction of the fluence with N.

In the last years, the Burst Mode (BM) ablation was introduced, consisting of using groups of several sub-pulses (the so-called bursts) with time separations shorter than 1 microsecond (Gattass et al., 2006). Consequently, when processing with bursts instead of trains of pulses, two additional parameters should be taken into account: the number of sub-pulses constituting the bursts and their time separations.

Although some studies have been performed to compare the efficiency of ablation process in BM and NPM, few researches have been focused on the dependence of ablation threshold on bursts features. Gaudiuso et al., 2016, performed a systematic study on the laser ablation of silicon with bursts of 200 fs pulses with delays ranging from 0.5 ps to 4 ps and from 0.5 ns to 4 ns, respectively. Here, the change of the burst damage threshold with the time separation between sub-pulses was investigated and a substantial invariance of the threshold fluence was found for delays shorter than 4 ps. A significant increase of the damage threshold was observed when the separation time was longer than 0.5 ns, so showing the existence of two different ablation mechanisms depending on the burst features.

In this work, we have carried out an experimental investigation of laser ablation with burst of 650 fs, 1030nm sub-pulses with a time separation of 1.5 ps, while keeping the laser repetition rate at 100 kHz. The ablation thresholds in BM and NPM were measured and compared.

2. Experimental Set-up

The ultrafast laser source used for this study is a high-average-power, high-repetition-rate fiber chirped pulse amplification (CPA) system (mod. Sci-series) from Active Fiber Systems GmbH. It delivers a linearly polarized laser beam with Gaussian profile (M^2~1.25) at a wavelength of 1030 nm, with tunable pulse duration in the range 650 fs – 20 ps. The maximum achievable pulse energy and average laser power are 100 µJ and 50 Watt, respectively, in a tunable range of repetition rates from 50 kHz to 10 MHz. An external acousto-optic modulator allows picking from single to any desired number N of pulses at the selected repetition rate. In this work, the laser has been operated with the shortest pulse duration of 650 fs and at a fixed repetition rate of 100 kHz.

The laser beam has been used either in Normal Pulse Mode or in Burst Mode. Bursts have been generated by using an array of five birefringent calcite crystals which split the linearly polarized 650 fs pristine pulses exiting from the laser source into n sub-pulses of same time duration and equal fractioned energy. The

number *n* depends on how the optical axes of the crystals are oriented with respect to the polarization of the incident pulses. According to the orientation of each crystal of the array, it is possible to change the number of sub-pulses in the burst, from 2 up to 32. More details on the burst generator set-up can be found in Dromey et al., 2007 and Zhou et al., 2007.

Experiments consisted in producing several craters by laser ablation on polished stainless steel (AISI304) targets either by focusing trains of undivided laser pulses of energy E_p in NPM or bursts with equivalent amount of energy E_b in BM. The laser beam was focused using a 100-mm focal length plano-convex lens at normal incidence to the targets surface. Samples were placed on the lens focal plane and translated through a motorized XY linear stage. Ablation was performed in ambient air without any gas shielding.

Bursts with different number of sub-pulses (n =2, 4, 8, 16 and 32), with time separations Δt=1.5 ps between sub-pulses, were used. For each burst configuration, the burst energy E_b was varied in the range 5-25 μJ.

The number of pulses *N* impinging onto the same spot of the sample in NPM or, equivalently, the number of bursts in BM, was also changed in the range from 50 to 1600.

Table 1 reports a summary of the set of parameters used for ablation experiments.

Table 1. Summary of investigated working parameters in BM.

Number of sub-pulses in the burst, *n*	2	4	8	16	32
Burst energy, E_b	5 – 7.5 – 10 – 12.5 – 15 – 20 – 25 μJ				
Number of bursts, *N*	50 – 100 – 200 – 400 – 800 – 1600				

In order to estimate the ablation threshold for each process condition, the diameter of the craters was measured with an optical microscope Nikon Eclipse ME600.

3. Results and discussion

The method proposed by Liu, 1982, enables estimating the laser ablation threshold by assuming a laser beam with a Gaussian spatial distribution and the following relationship between the threshold fluence F_{th} and the diameter *D* of the ablated crater:

$$D^2 = 2w^2 \ln\left(\frac{F_0}{F_{th}}\right) \quad (1)$$

where *w* is the laser spot radius on the sample surface and F_0 is the peak laser fluence given by:

$$F_0 = \frac{2E}{\pi w^2} \quad (2)$$

E indicates the energy of the undivided pulses E_p in NPM or the sub-pulse energy E_{sp} in BM, respectively. From Eq. 1, the squared diameters increase linearly with $ln(F_0)$, then the ablation threshold fluence can be obtained by extrapolating the value of fluence corresponding to a laser ablation crater with zero diameter. In Fig. 1 (a) the experimental data evaluated in NPM for different values of fixed *N* are showed, while in Fig. 1

(b) the experimental data obtained with burst of n=16 sub-pulses and time separation of 1.5 ps are plotted. Similar trends were found for all the experimental conditions summarized in Table 1.

Each point in the plots represents the average value of five replicas of craters performed in the same experimental condition, while the error bar is associated to its standard deviation.

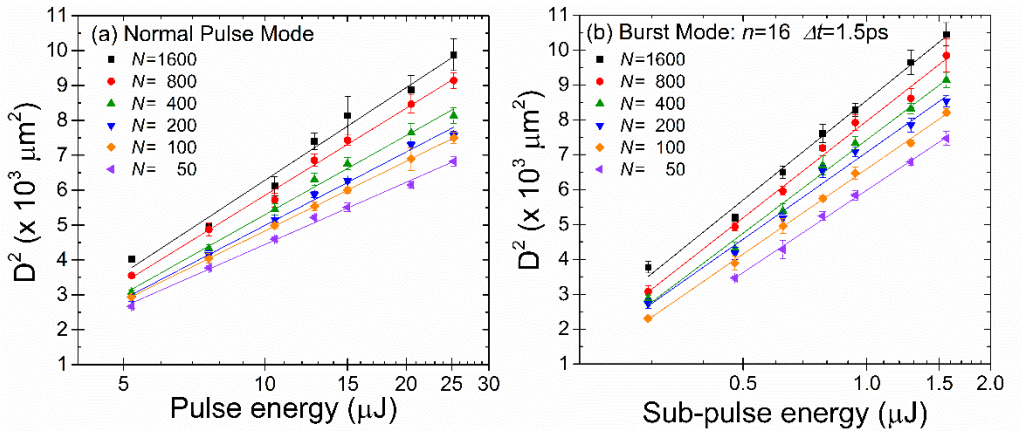

Fig. 1. (a) Semi-log plot of squared diameters of the ablated craters vs pulse energy in NPM for stainless steel when irradiated with N = 50, 100, 200, 400, 800, 1600 pulses.; (b) Semi-log plot of squared diameters vs sub-pulse energy for n=16 sub-pulses in the bursts with a time separation of 1.5 ps for stainless steel when irradiated with N = 50, 100, 200, 400, 800, 1600 bursts.

For both NPM and BM, all fits of Fig. 1 show a linear dependence of the squared diameters on the pulse or burst energy for each value of investigated N. This trend is confirmed for all the combinations of explored parameters reported in Table 1. Furthermore, the fitting lines drawn in semi-log plot are almost parallel, thus indicating that uniform focusing conditions were kept during the experiments, being the slope of the regression lines related to the beam spot size on the target surface. The estimated average value for the spot radius is 43.1 ± 3.8 μm. On the other hand, the threshold fluence was calculated from the intercept of the linear fits with the x-axis.

The evaluated threshold fluences are shown in Fig. 2 as a function of the total number of sub-pulses N_{tot}=N·n irradiating the same spot, in order to study the influence of BM processing on the incubation effect. For the sake of clarity, Fig. 2 shows the trend of the threshold fluence for BM processing with 8 and 32 sub-pulses. The threshold fluence in case of NPM (black squares) is reported for comparison. In the latter case N_{tot} corresponds to N.

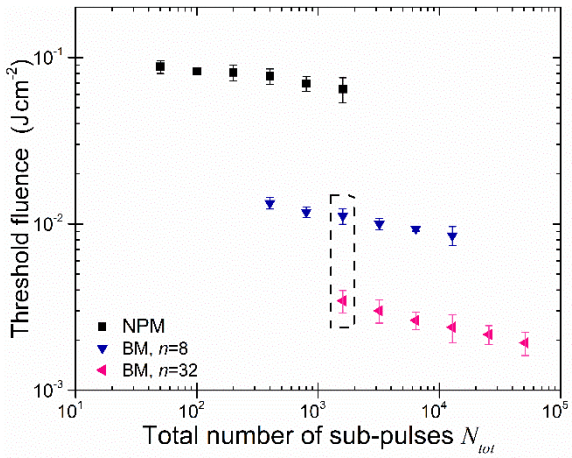

Fig. 2. Semi-log plot of threshold fluence vs the total number of sub-pulses $N_{tot}=N\cdot n$. The time separation between consecutive sub-pulses in the burst is 1.5 ps. The black squares show the threshold fluence for NPM.

A decrease of the threshold fluence is clearly observed as the total number N_{tot} increases for both NPM and BM. This result is ascribed to incubation effect (Neuenschwander et al., 2014, Chowdhury et al., 2003).

In Fig. 2 it is evident that the decrease of damage threshold in BM is mainly due to the growth of the number of sub-pulses constituting the burst, rather than the number of bursts itself. In fact, considering data referred to the same burst features, i.e. same number *n* of sub-pulses, the decrease of the threshold fluence with the number of burst *N* is relatively small compared to the case when *N* is fixed and the number of sub-pulses in the bursts *n* is increased. For instance, for *N*=50, by increasing the number of pulse splitting from *n*=8 to *n*=32, a considerable reduction of 74% of the threshold fluence is found. Therefore, for a fixed total number of sub-pulses N_{tot} different damage threshold values were found for each combination of *N* and *n*. This is better highlighted in Fig. 2 for N_{tot}=1600 (points inside the dashed rectangle).

According to the incubation model introduced by Jee et al., the relation between the threshold fluence F_{th} per *N* pulses and the number of applied pulses *N* is given by:

$$F_{th}(N) = F_{th}(1)\cdot N^{(S-1)} \qquad (3)$$

Here, $F_{th}(N)$ is the threshold fluence for *N* pulses, $F_{th}(1)$ is the threshold fluence for a single shot, while *S* is the incubation coefficient and describes the strength of incubation effect. This model describes the decreasing behavior of the ablation threshold in NPM and it returns one single value of threshold fluence once the number *N* is fixed.

However, according to our results such a model would be inapplicable to BM processing, since it does not take into account the possibility that the threshold fluence varies according to the burst feature, as shown in the Fig. 2.

4. Conclusion

In order to investigate incubation effect in Burst Mode processing, craters were generated with bursts of 2 up to 32 sub-pulses with time separation of 1.5ps. The study was conducted with 1030 nm wavelength ultrashort pulses of 650 fs at a repetition rate of 100 kHz.

Threshold fluence values were determined with the Liu method, by the measuring the crater diameters and analyzing their trend as a function of the sub-pulse energy. For comparison, analogous experiments have been carried out with undivided pulses in the so-called Normal Pulse Mode, in the same experimental conditions.

For both processing modes, it was found that the threshold fluence decreases when increasing the total number of sub-pulses.

However, while the incubation model introduced by Jee et al. well describes the data obtained in NPM, it is unable to predict incubation of the damage threshold in BM processes. Indeed, it is based on the assumption that only one value of the threshold fluence applies for each total amount N_{tot} of sub-pulses impinging on the sample surface. While our experimental results clearly showed that as many values of threshold fluence can be found as the combinations of number of bursts N and number of sub-pulses within each burst n giving the same N_{tot}.

References

Bonse, J., Baudach, S., Krüger, J., Kautek, W., Lenzner, M., 2002. Femtosecond laser ablation of silicon-modification thresholds and morphology, Applied Physics A 74, p. 19.

Breitling, D., Ruf, A., Dausinger, F., 2004. Fundamental aspects in machining of metals with short and ultrashort laser pulses, Proceedings of SPIE 5339.

Chowdhury, I. H., Xu, X., Weiner, A. M., 2003. Ultrafast pulse train micromachining, Proceedings of SPIE 4978, 138.

Di Niso, F., Gaudiuso, C., Sibillano, T., Mezzapesa, F. P., Ancona, A., Lugarà, P. M., 2014. Role of heat accumulation on the incubation effect in multi-shot laser ablation of stainless steel at high repetition rates, Optics Express 22, p. 12200.

Dromey, B., Zepf, M., Landreman, M., O'Keeffe, K., Robinson, T., Hooker, S. M., 2007. Generation of a train of ultrashort pulses from a compact birefringent crystal array, Applied Optics 46, p. 5142.

Gattass, R. R., Cerami, L. R., Mazur, E., 2006. Micromachining of bulk glass with bursts of femtosecond laser pulses at variable repetition rates, Optics Express 14, p.5279.

Gaudiuso, C., Kämmer, H., Dreisow, F., Ancona, A., Tünnermann, A., Nolte, S., 2016. Ablation of silicon with bursts of femtosecond laser pulses, Proceedings of SPIE 9041.

Gómez, D., Goenaga, I., 2006. On the incubation effect on two thermoplastics when irradiated with ultrashort laser pulses: broadening effects when machining microchannels, Applied Surface Science 253, p. 2230.

Jee, Y., Becker, M. F., Walser, R. M., 1988. Laser-induced damage on single-crystal metal surfaces, Journal of the Optical Society of America B 5, p. 648.Nathala, C. S. R., Ajami, A., Husinsky, W., Farooq, B., Kudryashov, S. I., Daskalova, A., Bliznakova, I., Assion, A., 20156. Ultrashort laser pulse ablation of copper, silicon and gelatin: effect of the pulse duration on the ablation thresholds and the incubation coefficients, Applied Physics A 122, p. 9625.

Liu, J. M., 1982. Simple technique for measurements of pulsed Gaussian-beam spot sizes, Optics Letters 7, p. 196.

Machado, L. M., Samad, R. E., de Rossi, W., Vieira, N. D. Jr., 2012. D-Scan measurements of ablation threshold incubation e ect for ultrashort laser pulses, Optics Express, 20, p. 4114.

Mannion, P. T., Magee, J., Coyne, E., O'Connor, G. M., Glynn, T. J., 2004. The effect of damage accumulation behaviour on ablation thresholds and damage morphology in ultrafast laser micro-machining of common metals in air, Applied Surface Science 233, p. 275.

Neuenschwander, B., Jaeggi, B., Schmid, M., Dommann, A., Neels, A., Bandi, T., Hennig, G., 2013. Factors controlling the incubation in the application of ps laser pulses on copper and iron surfaces, Proceedings of SPIE 8607.

Neuenschwander, B., Jaeggi, B., Schmid, M., Hennig, G. , 2014. Surface structuring with ultra-short laser pulses: Basics, limitations and needs for high throughput, Physics Procedia 56, p. 1047.

Ren, Y., Cheng, C. W., Chen, J. K., Zhang, Y., Tzou, D. Y., 2013. Thermal ablation of metal films by femtosecond laser bursts, International Journal of Thermal Sciences 70, p. 32.

Zhou, S., Ouzounov, D., Li, H., Bazarov, I., Dunham, B., Sinclair, C., Wise, F. W. , 2007. Efficient temporal shaping of ultrashort pulses with birefringent crystals, Applied Optics 46, p. 8488.